# Damage-based fracture with electro-magnetic coupling

P. Areias[ł⋆*], H.G. Silva[ł], M. Bezzeghoud[ł], N. Van Goethem[+]

19th September 2011

[ł]Departamento de Física
Universidade de Évora
Colégio Luís António Verney
Rua Romão Ramalho, 59
7002-554 Évora, Portugal

[+]CMAF, Universidade de Lisboa, Faculdade de Ciências,
Departamento de Matemática
Centro de Matemática e Aplicacações Fundamentais
Av. Prof. Gama Pinto 2, 1649-003 Lisboa, Portugal
[⋆]ICIST

**Abstract**

A coupled elastic and electro-magnetic analysis is proposed including finite strains and damage-based fracture. Piezo-electric terms are considered and resulting partial differential equations include a non-classical wave equation due to the specific constitutive law. The resulting wave equation is constrained and, in contrast with the traditional solutions of the decoupled classical electro-magnetic wave equations, the constraint is directly included in the analysis. The absence of free current density allows the explicitation of the magnetic field rate as a function of the electric field and therefore removal of the magnetic field from the list of unknowns. A Lagrange multiplier field is introduced to exactly enforce the divergence constraint, forming a three-field variational formulation. No vector-potential is required or mentioned, eliminating the need for gauges. The classical boundary conditions of electromagnetism are specialized and a new general boundary condition involving the electric field is obtained. A specific boundary finite element is introduced to deal with this boundary condition. The spatial discretization makes use of mixed bubble-based (MINI-like) finite elements with displacement, electric field and Lagrange multiplier degrees-of-freedom. Two verification examples are presented with very good qualitative conclusions and mesh-independence.

KEYWORDS: Electro-magnetism, Maxwell's equations, elasticity, piezo-electricity

[*]Corresponding Author. ISI search: areias p*; email: pmaa@uevora.pt, pareias@civil.ist.utl.pt, Ph.: +351 96 3496307, URL: http://evunix.uevora.pt/~pmaa/

# 1 Introduction

Fundamental theoretical contributions for the analysis of continuum elastic dielectrics are Lax and Nelson [16] and Maugin [20]. The latter text contains many contributions with a detail beyond what is intended with this work. The purpose of it is to inaugurate our approach to electro-magnetic and elasticity coupling implemented with mixed finite elements to deal with fracture (in finite strains). Piezo-electricity is also included, but mainly as a constitutive ingredient. Recent discussions on this topic, also with a continuum approach, are the works of Ericksen (cf. [8, 9]) and Dorfmann and Ogden [7] albeit limited to strict dielectrics (without the magnetic field). Numerical calculations are sparse and mainly limited to magnetostatics (see, for example [6]) and piezo-electricity. M. Kuna [15] performed a theoretical and experimental review of piezo-electricity with classical fracture mechanics. In [14], the same author used a electromechanical contour integral to calculate energy release rates.

We perform finite strain simulations of electro-magnetic fields including piezo-electricity. The total stress contains the Cauchy stress, the Maxwell stress, the piezo-electric stress and the polarization stress. The piezoelectric effect is characterized as a coupling between the electric polarization of a given material and the (mechanical) stress field. It is crucial in sensors, actuators, smart materials among others. There is a significant variety of piezoelectric materials: crystals, e.g. quartz; ceramics, e.g. lead zirconate titanate (PZT); polymers, e.g. polyvinylidene fluoride (PVDF).

Taking into account that materials are subjected to frequent mechanical actions it is of fundamental importance the study of fracture, in order to estimate their reliability to device applications. For that reason, many works have been focused on this topic, for a recent review the reader is referred to [15]. Interestingly, the majority of them only consider the electrostatic limit where the coupling of the electric and magnetic fields (present in Maxwell's equations) can be neglected and the analysis can be restricted to the electrical field. Obviously, this constitutes an overall simplification to the problem since in this case the electric field (vector), $\boldsymbol{e}$, can be calculated from the divergence of the electrical potential (scalar), $\phi$, reducing a $n$-dimensional problem (2 or 3, typically) to a one-dimensional one.

The remaining of this paper is composed of four sections. Section 2 contains the basic premises of our work, as well as original derivations for the weak form and boundary conditions. Section 3 briefly summarizes the discretization proposal, the mixed finite element and a special boundary finite element to enforce the newly derived boundary condition in terms of the electric field. Section 4 presents two numerical applications where the new technique is very successfully tested and in section 5 some conclusions are drawn.

# 2 Governing equations

## 2.1 Maxwell and equilibrium equations

We consider a linear elastic material with a damage evolution law, equilibrium with moderately large strains (ensuring the validity of Hooke's law) and the classical electrodynamics of continua (cf. [16, 20]).

The considered governing equations consist of:

- Cauchy equations of motion using the electromagnetic force as the only volume force.

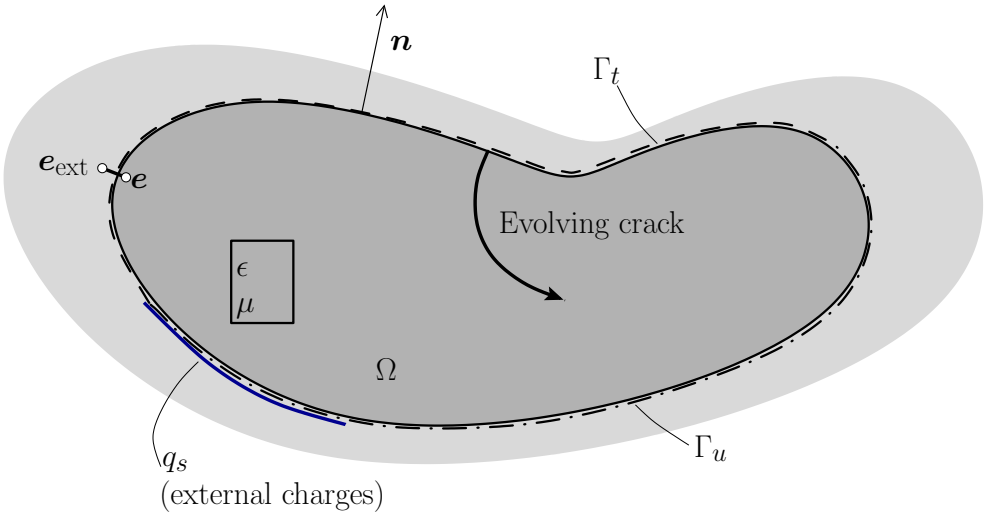


Figure 1: Relevant ingredients for the coupled equilibrium/electromagnetic problem (current configuration). The electric field's equation holds in the interior and in the exterior of $\Omega$ with matching of the external and internal values on every portion of the boundary where $q_s = 0$.

- Mass conservation.
- Maxwell's equations in S.I. units for dielectrics, in the absence of free charges and currents.
- Linear constitutive equations of electromagnetism, stress-strain relations and piezoelectricity.

Figure 1 shows the idealization of the typical problem to be solved and the three types of boundary conditions (essential for the displacement unknown and electric field and natural boundary conditions).

The mass conservation principle for an impermeable continuum (open set $\Omega$) is concisely given by:

$$\frac{\partial(J\rho)}{\partial t} \quad = \quad 0 \quad \text{in} \quad \Omega \tag{1}$$

where $\rho$ is the spatial mass density and $J = \det \boldsymbol{F}$ where $\boldsymbol{F}$ is the deformation gradient (cf. [22]).

The Cauchy equation of motion and Cauchy Lemma read:

$$\boldsymbol{\nabla} \cdot \boldsymbol{\sigma}^T + \boldsymbol{f} = \rho \ddot{\boldsymbol{u}} \quad \text{in} \quad \Omega \tag{2}$$

$$\boldsymbol{\sigma n} = \bar{\boldsymbol{t}} \quad \text{in} \quad \Gamma_t \tag{3}$$

where $\boldsymbol{\sigma}$ is the Cauchy stress tensor, $\boldsymbol{u}$ is the displacement vector and $t \in [0, T]$ is the time variable (not

to be mistaken with $\bar{\boldsymbol{t}}$, the prescribed stress vector) and the term $\boldsymbol{f}$ is the body-force field. This is of course standard (e.g. [22, 19]) and shown here for completeness. A useful notion in elastic dielectricity is the one of total stress, here denoted as $\boldsymbol{\sigma}^{\star}$ which allows the rewriting of (2) as:

$$\boldsymbol{\nabla} \cdot \boldsymbol{\sigma}^{\star^T} = \rho \ddot{\boldsymbol{u}} \tag{4}$$

In particular, we consider $\rho \ddot{\boldsymbol{u}} = \boldsymbol{0}$ in remaining of this work. Note that, according to our notation, $\sigma_{ij}$ is the Cauchy stress component at facet $j$ with the direction $i$. Maxwell's equations in classical form[1] in a domain $\Omega$ (cf. [10, 12, 9, 21]) are concisely written as:

$$\boldsymbol{\nabla} \times \boldsymbol{e} + \dot{\boldsymbol{b}} = \boldsymbol{0} \quad \text{in} \quad \Omega \tag{5}$$

$$\boldsymbol{\nabla} \cdot \boldsymbol{b} = 0 \quad \text{in} \quad \Omega \tag{6}$$

$$\boldsymbol{\nabla} \times \boldsymbol{h} - \dot{\boldsymbol{d}} = \boldsymbol{J}_f \quad \text{in} \quad \Omega \tag{7}$$

$$\boldsymbol{\nabla} \cdot \boldsymbol{d} = q_f \quad \text{in} \quad \Omega \tag{8}$$

where $\boldsymbol{e}$ is the electrical field, $\boldsymbol{b}$ is the magnetic field, $\boldsymbol{h}$ is the magnetic field strength and $\boldsymbol{d}$ is the electric displacement current (see, e.g. [10]). The terms in the right-hand sides of (7) and (8) are the free external current and charge, respectively, as related by the continuity equation: $\dot{q}_f + \boldsymbol{\nabla} \cdot \boldsymbol{J}_f = 0$.

It is noticeable that the validity of (5-8) for a continuum described in the spatial configuration is shown by Lax and Nelson [16]. Here, the following notation is adopted (see also [16]):

$$\dot{\bullet} = \frac{\partial \bullet}{\partial \mathrm{t}} \tag{9}$$

The inclusion of piezo-electricity in the system (5-8) can made by means of the polarization vector or directly by introduction in a constitutive law for $\boldsymbol{d}$. The latter is used here. As a matter of fact, for piezo-electric materials under consideration, we introduce a linear relation between the electric displacement, the electric field and the strain $\boldsymbol{\varepsilon}$[2]:

$$\boldsymbol{d} = \epsilon \left( \boldsymbol{e} - \mathscr{I} : \boldsymbol{\varepsilon} \right) \tag{10}$$

where $\epsilon$ is the electrical permitivity[3] of a given material and $\mathscr{I}$ is the piezo-electric third-order tensor.

[1] S.I. units are adopted and lower-case is used for spatial quantities.

[2] We purposely leave "strain" undefined for now.

[3] As a first approach we assume a scalar permitivity for simplicity.

Note that this definition agrees with the interpretation of Dorfmann and Ogden ([7]). that "*the difference* $\boldsymbol{d} - \epsilon \boldsymbol{e}$ *[...] is a material-dependent property that has to be given by a constitutive equation.*" Another paper with the same interpretation is Ponte Castañeda and Siboni [23]. It is also noticeable that the approach of M. Kuna in [14] can be re-cast in this form.

For homogeneous linear isotropic continua, for which Lorentz aether relations hold[4], we can write (7) and (8) as:

$$\boldsymbol{\nabla} \times \boldsymbol{b} = \mu \boldsymbol{J}_f + \mu\varepsilon \left( \dot{\boldsymbol{e}} - \mathscr{I} : \dot{\boldsymbol{\varepsilon}} \right) \quad \text{in} \quad \Omega \tag{11}$$

$$\epsilon \boldsymbol{\nabla} \cdot \left( \boldsymbol{e} - \mathscr{I} : \boldsymbol{\varepsilon} \right) = q_f \quad \text{in} \quad \Omega \tag{12}$$

where $\mu$ is the magnetic permeability. Both $\epsilon$ and $\mu$ can be related to the corresponding vacuum constants. A direct manipulation results in the following second-order system[5]:

$$\boldsymbol{\nabla} \times \left( \boldsymbol{\nabla} \times \boldsymbol{e} \right) + \mu \dot{\boldsymbol{J}}_f + \mu\varepsilon \left( \ddot{\boldsymbol{e}} - \ddot{\boldsymbol{p}} \right) = \boldsymbol{0} \tag{13}$$

$$\boldsymbol{\nabla} \cdot \left( \boldsymbol{e} - \boldsymbol{p} \right) = \frac{q_f}{\epsilon} \tag{14}$$

with $\boldsymbol{p} = \mathscr{I} : \boldsymbol{\varepsilon}$ (do not confuse $\boldsymbol{p}$ with the polarization field). It is clear that $\nabla \cdot \boldsymbol{b} = 0$ is trivially satisfied in $[0, T]$ provided $\left( \boldsymbol{\nabla} \cdot \boldsymbol{b} \right)(0) = \boldsymbol{0}$ is satisfied. Moreover, the reader can verify that, contrary to traditional derivations in electromagnetic wave propagation, no Laplacian of $\boldsymbol{e}$ emerges in (13) since the classical condition $\boldsymbol{\nabla} \cdot \boldsymbol{e} = 0$ does not hold, due to the piezoelectric term in (14).

After direct specialization of the general boundary conditions (cf. [16]), a final set of boundary conditions for piezoelectricity and electromagnetic coupling is obtained:

$$\left[ \left[ \frac{1}{\mu} \boldsymbol{b} - \dot{\boldsymbol{u}} \times \boldsymbol{d} \right] \right] \times \boldsymbol{n} = \boldsymbol{J}_s \tag{15}$$

$$\left[ \left[ \boldsymbol{e} + \dot{\boldsymbol{u}} \times \boldsymbol{b} \right] \right] \times \boldsymbol{n} = \boldsymbol{0} \tag{16}$$

$$\left[ \left[ \epsilon \left( \boldsymbol{e} - \boldsymbol{p} \right) \right] \right] \cdot \boldsymbol{n} = q_s \tag{17}$$

$$\left[ \left[ \boldsymbol{b} \right] \right] \cdot \boldsymbol{n} = 0 \tag{18}$$

We use the notation $[[\bullet]]$ for the "jump" of $\bullet$: the difference between the *external* and *internal* values of $\bullet$ (see figure 1). The following boundary conditions for (13-14) are adopted for the whole $\Gamma$ in the case of *null external fields* (cf. [21, 18]):

$$\boldsymbol{n} \cdot \left( \boldsymbol{p} - \boldsymbol{e} \right) = \frac{q_s}{\epsilon} \quad \text{in} \quad \Gamma \tag{19}$$

$$\boldsymbol{e} \times \boldsymbol{n} = -(\dot{\boldsymbol{u}} \times \boldsymbol{b}) \times \boldsymbol{n} \tag{20}$$

[4] If spatial coordinates are used, as sharply recalled by Ericksen [8].

[5] It can be shown that $\boldsymbol{\nabla} \cdot \boldsymbol{b} = 0$ is trivially satisfied if $\boldsymbol{b}_0 = \boldsymbol{0}$, i.e. the initial value of $\boldsymbol{b}$ is identically zero.

It can be proven that the condition $[[\boldsymbol{b}]] \cdot \boldsymbol{n} = 0$ is satisfied as a consequence of (20). Contrary to the charge surface density, $q_s$, the surface current density $\boldsymbol{J}_s$ is not directly imposed in this framework (see also the recent paper by Linder *et al.* [18]). A simple adaptation is possible but it will not be pursued here. A trivial combination of (19) and (20) reads

$$\boldsymbol{e} = \left[ (\boldsymbol{p} + \dot{\boldsymbol{u}} \times \boldsymbol{b}) \cdot \boldsymbol{n} - \frac{q_s}{\epsilon} \right] \boldsymbol{n} - \dot{\boldsymbol{u}} \times \boldsymbol{b} \quad \text{in} \quad \Gamma \tag{21}$$

To the best knowledge of the authors, this condition for $\boldsymbol{e}$ in $\Gamma$ has not been presented before in the specialized literature. Note that the complete $\boldsymbol{e}$ is specified at $\Gamma$, in contrast with what occurs in piezo-electric reports. Typically (see [18]) the unknown field is $\boldsymbol{d}$ and not $\boldsymbol{e}$ since the magnetic field is seldom included in numerical simulations. For dielectrics (considered in this work) it follows that $\boldsymbol{J}_f = \boldsymbol{0}$ and $q_f = 0$ (see, for example, the book of Maugin [20] page 157). As a strain tensor we adopt (see Ogden [22] eq. 2.2.82 page 118 with $m = 2$) the following Eulerian tensor:

$$\boldsymbol{\varepsilon} = \frac{1}{2} \left( \boldsymbol{V}^2 - \boldsymbol{I} \right) \tag{22}$$

with $\boldsymbol{V}$ being the left stretch tensor, ensures that third derivatives of strain with respect to $\boldsymbol{V}$ are zero (advantage of this will be taken later in the linearization stage). The constitutive law for the *total* stress is given as[6]:

$$\boldsymbol{\sigma}^\star = \underbrace{(1-f)\mathscr{C} : \boldsymbol{\varepsilon}}_{\boldsymbol{\sigma}_e} + \underbrace{\frac{1}{\mu}\boldsymbol{b} \otimes \boldsymbol{b} + \epsilon \boldsymbol{e} \otimes \boldsymbol{e} - \frac{1}{2}\left( \epsilon \|\boldsymbol{e}\|^2 + \frac{1}{\mu}\|\boldsymbol{b}\|^2 \right) \boldsymbol{I}}_{\boldsymbol{\sigma}_M} + \underbrace{\epsilon \boldsymbol{e} \cdot \mathscr{I}}_{\boldsymbol{\sigma}_{PE}} \underbrace{-\epsilon \boldsymbol{p} \otimes \boldsymbol{e}}_{\boldsymbol{\sigma}_S} \tag{23}$$

where $\boldsymbol{\sigma}_e$ is the elastic stress, $\boldsymbol{\sigma}_M$ is the Maxwell stress, $\boldsymbol{\sigma}_{PE}$ is the piezo-electric stress and $\boldsymbol{\sigma}_S$ is the polarization stress (see also [20], where Gaussian units are adopted). Note that the electric field already accounts for the piezo-electric effect in the global PDE in (13) and hence the reciprocal piezo-electric law is enforced at the global level. The term $\boldsymbol{\sigma}_S$ of course results from the product $\boldsymbol{d} \otimes \boldsymbol{e}$ (see [25]). Note that the transfer of body forces to the total stress has been an implicit practice in Physics literature (the book by Maugin [20] is particularly diffuse in this topic since only the non-symmetric part of the Cauchy stress is left as a body force term) and is explicit, for example, in the paper by Vu, Steinmann and Possart (cf. [25] equations (12) and (13)). In (23), the elastic stress contains the term $(1-f)$ where $f$ is the void fraction, a constitutive variable accounting for material softening. We use a phenomenological model (see also [17]) which is sufficient for this work's purpose. Also included in (23) is the third order piezo-electric tensor $\mathscr{I}$. Damage modeling includes a loading function and the loading/unloading conditions. The corresponding void fraction loading function is:

$$\varphi(\boldsymbol{\varepsilon}) = (1-f)\varepsilon_1 - \varepsilon_{\max} \tag{24}$$

[6] In contrast with Chapter 4 of [20], we do not include electro-magnetic terms in the body forces.

where $\varepsilon_1$ is the maximum principal strain and $\varepsilon_{\max}$ is the maximum principal strain attained during the loading history at a given point. The following loading/unloading conditions are used for this Rankine-type model:

$$\begin{aligned} \varphi(\boldsymbol{\varepsilon}) &\leq 0 && (25)\\ \dot{f}\varphi(\boldsymbol{\varepsilon}) &= 0 && (26)\\ \dot{f} &\geq 0 && (27) \end{aligned}$$

The final equations to integrate are therefore dependent on $\boldsymbol{\sigma}$:

$$c^2\left[\boldsymbol{\nabla}\times(\boldsymbol{\nabla}\times\boldsymbol{e})\right]+(\ddot{\boldsymbol{e}}-\ddot{\boldsymbol{p}})=\mathbf{0} \quad \text{in} \quad \Omega \tag{28}$$

$$\boldsymbol{\nabla}\cdot\boldsymbol{\sigma}^{\star T}=\mathbf{0} \quad \text{in} \quad \Omega \tag{29}$$

$$\boldsymbol{\nabla}\cdot(\boldsymbol{e}-\boldsymbol{p})=0 \quad \text{in} \quad \Omega \tag{30}$$

$$\boldsymbol{e}=\left[(\boldsymbol{p}+\dot{\boldsymbol{u}}\times\boldsymbol{b})\cdot\boldsymbol{n}-\frac{q_s}{\epsilon}\right]\boldsymbol{n}-\dot{\boldsymbol{u}}\times\boldsymbol{b} \quad \text{in} \quad \Gamma \tag{31}$$

$$\boldsymbol{\sigma}\boldsymbol{n}=\bar{\boldsymbol{t}} \quad \text{in} \quad \Gamma_t \tag{32}$$

$$\boldsymbol{u}=\overline{\boldsymbol{u}} \quad \text{in} \quad \Gamma_u \tag{33}$$

with $c^2=1/(\mu\epsilon)$ being the square of the light velocity in the continuum. Note that no body forces are employed since the electro-magnetic field effect on the forces is completely included in $\boldsymbol{\sigma}^\star$ (in equation (23)) and the Cauchy lemma retains its original form (in equation 32). The weak form of the above equations is obtained by using a Lagrange multiplier field, $\lambda\equiv\lambda(\boldsymbol{x})$ and performing the customary projections and use of Green's theorem. We introduce the spaces for the *test* functions $\mathscr{V}_u=\{\delta u_i\in H^1(\Omega)|\delta\boldsymbol{u}=\mathbf{0} \quad \text{in} \quad \Gamma_u\}$, $\mathscr{V}_d=\{\delta d_i\in H^1(\Omega)|\delta\boldsymbol{d}=\mathbf{0} \quad \text{in} \quad \Gamma\}$ and $\mathscr{P}=\{\delta\lambda\in L^2(\Omega)|\delta\lambda=0 \quad \text{in} \quad \Gamma\}$ and the *sets* for the trial functions $\mathscr{D}_u=\{u_i\in H^1(\Omega)|u_i=\overline{u}_i \quad \text{in} \quad \Gamma_u\}$, $\mathscr{D}_d=\{e_i\in H^1(\Omega)|e=\overline{e}_i \quad \text{in} \quad \Gamma\}$ and $\mathscr{P}$ (the Lagrange multiplier *space* for test functions and *set* for trial functions coincide). The problem statement in weak form reads: find $\boldsymbol{u}\in\mathscr{D}_u$, $\boldsymbol{e}\in\mathscr{D}_e$, and $\lambda\in\mathscr{P}$ such that the following holds (see [11] for this nomenclature and symbols):

$$\int_\Omega c^2(\boldsymbol{\nabla}\times\boldsymbol{e})\cdot(\boldsymbol{\nabla}\times\delta\boldsymbol{d})\mathrm{d}\Omega+\int_\Gamma c^2\underbrace{[(\boldsymbol{\nabla}\times\boldsymbol{e})\times\delta\boldsymbol{d}]\cdot\boldsymbol{n}}_{-[(\boldsymbol{\nabla}\times\boldsymbol{e})\times\boldsymbol{n}]\cdot\delta\boldsymbol{d}=0}\mathrm{d}\Gamma+\int_\Omega(\ddot{\boldsymbol{e}}-\ddot{\boldsymbol{p}})\cdot\delta\boldsymbol{d}\mathrm{d}\Omega$$
$$+\int_\Omega\boldsymbol{\sigma}:\nabla^s\delta\boldsymbol{u}\,\mathrm{d}\Omega-\int_{\Gamma_t}\bar{\boldsymbol{t}}\cdot\delta\boldsymbol{u}\mathrm{d}\Gamma_t$$
$$+\int_\Omega\lambda\delta\left[\boldsymbol{\nabla}\cdot(\boldsymbol{e}-\boldsymbol{p})\right]\mathrm{d}\Omega$$
$$\int_\Omega\delta\lambda\left[\boldsymbol{\nabla}\cdot(\boldsymbol{e}-\boldsymbol{p})\right]\mathrm{d}\Omega\;=\;0\qquad(34)$$

$\forall\delta\boldsymbol{d}\in\mathscr{V}_d$, $\forall\delta\boldsymbol{u}\in\mathscr{V}_u$, $\forall\delta\lambda\in\mathscr{P}$.
The test functions $\delta\boldsymbol{d}$, $\delta\boldsymbol{u}$ and $\delta\lambda$ in (34) can be seen as variations of $\boldsymbol{d}$, $\boldsymbol{u}$ and $\lambda$, respectively. The $\delta-$variation of $\nabla(\bullet)$, where $\bullet$ is a generic spatial tensor and $\nabla$ is a spatial gradient is given as:

$$\delta\nabla\left(\bullet\right)=\nabla\delta\left(\bullet\right)-\nabla\left(\bullet\right)\nabla\delta\boldsymbol{u}\qquad(35)$$

This quantity is also used in the linearization process, required for the application of Newton's method of solution. We make use of the Acegen add-on [13] to the Mathematica software [24] to accomplish the derivation of the discretized equilibrium equations and corresponding linearization. The explicit expressions are omitted in this report. It is also noticeable that, in (34), the symmetric spatial gradient of $\delta\boldsymbol{u}$ is adopted: $\nabla^s\delta\boldsymbol{u}=\left[\nabla\delta\boldsymbol{u}+(\nabla\delta\boldsymbol{u})^T\right]/2$.

Initial conditions for (34) exist both for $\boldsymbol{u}$ and $\boldsymbol{e}$. In the present both initial values and corresponding time-derivatives are zero.

## 2.2 Piezo-electric matrix and orientation of axes

As a coupling between mechanical and electrical fields dependent on the orientation of a crystal. The invariance of the scalar $\boldsymbol{d}\cdot(\mathscr{I}:\boldsymbol{\varepsilon})$ (the reader can verify that this expression has units of energy) allows the writing of the following transformation of the piezo-electric matrix as a third-order tensor:

$$[\mathscr{I}]_{lmn}=[\boldsymbol{T}]_{il}\,[\boldsymbol{T}]_{mj}\,[\boldsymbol{T}]_{nk}\left[\widetilde{\mathscr{I}}\right]_{ijk}\qquad(36)$$

where the elements of $\boldsymbol{T}$ are obtained from two orthonormal basis $\boldsymbol{e}_j$ and $\widetilde{\boldsymbol{e}}_i$:

$$[\boldsymbol{T}]_{ij}=\widetilde{\boldsymbol{e}}_i\cdot\boldsymbol{e}_j=\cos\alpha_{ij}\qquad(37)$$

where $\alpha_{ij}$ are the internal angles between the basis vectors. It is obvious that minor-symmetry in the last two indices of $[\mathscr{I}]$ allows some computational savings in (36). It is here assumed that the tabulated piezo-electric properties correspond to the tensor components $\left[\widetilde{\mathscr{I}}\right]$ and $\alpha_{ij}$ are problem-dependent.

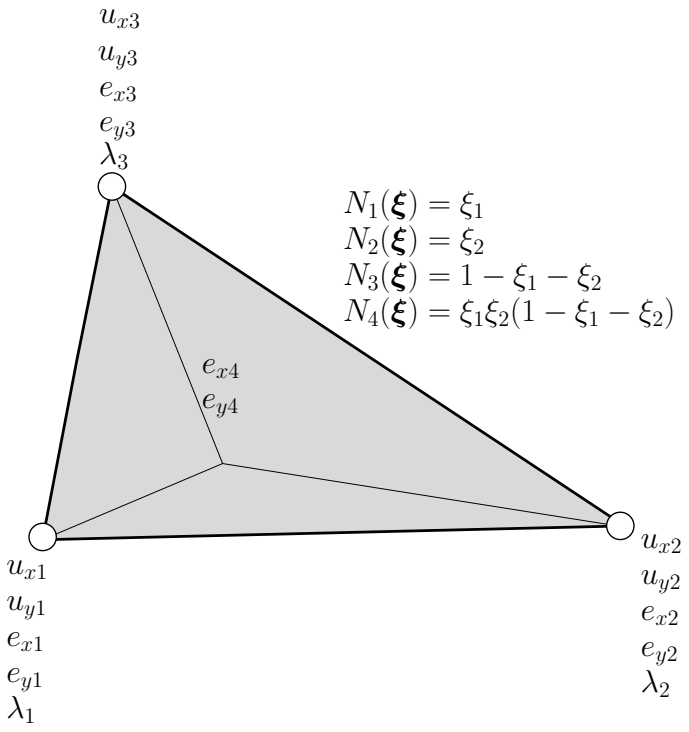


Figure 2: Use of MINI element ([5]) for the mixed $\boldsymbol{u} - \boldsymbol{e} - \boldsymbol{\lambda}$ problem.

# 3 Discretization and time integration

We use a variant of the MINI element by D. Arnold (cf. [5]) which was previously used for the Stokes equations to deal with the mixed problem (unknowns $\boldsymbol{u} - \boldsymbol{e} - \boldsymbol{\lambda}$). We also used it before for finite strain plasticity. Figure 2 shows the element degrees-of-freedom and the corresponding shape functions.

Time integration follows the *backward-Euler* method for first-order time integration applied both to degrees-of-freedom and their time-derivatives. If two consecutive time-steps are considered ($n$ and $n+1$), the following expression results for $\ddot{\boldsymbol{a}}_{n+1}$:

$$\ddot{\boldsymbol{a}}_{n+1} = \frac{\boldsymbol{a}_{n+1} - \boldsymbol{a}_n}{\Delta t^2} - \frac{\dot{\boldsymbol{a}}_n}{\Delta t} \tag{38}$$

where $\boldsymbol{a}$ contains degrees-of-freedom of all types ($\boldsymbol{u}$, $\boldsymbol{e}$ and $\lambda$). The velocity is obviously approximated as $\dot{\boldsymbol{a}}_{n+1} = (\boldsymbol{a}_{n+1} - \boldsymbol{a}_n)/\Delta t$. The magnetic field at step $n+1$ can therefore be obtained as:

$$\boldsymbol{b}_{n+1} = \boldsymbol{b}_n - \Delta t \boldsymbol{\nabla} \times \boldsymbol{e}_{n+1} \tag{39}$$

The magnetic field (39) is of course necessary for the boundary conditions and constitutive law

and must be stored as an history variable. If the previous value is known, then we can use the shape functions (and corresponding derivatives) to write the integrated boundary condition.

The relevant interpolated fields (with $h$ as the mesh characteristic length) in each element are obtained simply as:

$$\boldsymbol{u}^h = \sum_{K=1}^{3} N_K(\boldsymbol{\xi})\boldsymbol{u}_K \tag{40}$$

$$\boldsymbol{e}^h = \sum_{K=1}^{4} N_K(\boldsymbol{\xi})\boldsymbol{e}_K \tag{41}$$

$$\lambda^h = \sum_{K=1}^{3} N_K(\boldsymbol{\xi})\lambda_K \tag{42}$$

where $N_K(\boldsymbol{\xi})$ are the shape functions represented in figure 2. After time integration, these are the only degrees-of-freedom required to solve the coupled problem since $\boldsymbol{b}$ is written as a function of $\boldsymbol{e}$. We keep track of the previous step ($\boldsymbol{a}_n$ and $\dot{\boldsymbol{a}}_n$) which is sufficient to calculate $\ddot{\boldsymbol{a}}_n$ at the element level. The actual finite element implementation is too complex to be correctly and efficiently hand-coded and we resort to the Acegen software by J. Korelc ([13]) to accomplish this undertaking.

Boundary condition (31) requires a specific boundary finite element which makes use of strain to obtain $\boldsymbol{p}$ and the underlying continuum element to calculate $\boldsymbol{b}$. Boundary Lagrange multipliers (identified by the symbol $\chi$) are adopted to exactly enforce the condition. Figure (31) shows the adopted boundary element.

# 4 Numerical examples

## 4.1 Electric field pulling test: electromagnetic waves

Surface electric charges ($q_s$ in the above equations) cause electro-magnetic waves and, of course, stress waves (this is due to both the Maxwell stress term *and* the piezo-electric effect). Note that stress waves occur even *without* the inertial effect. With the purpose of obtaining a wave, we apply a time-constant electric charge at the surface of a straight bar and analyze the produced effect (in terms. Figure 4 shows the relevant quantities for this problem. A Lead Zirconate Titanate (PZT) material is considered, with properties shown in the same figure. Artificially large deformations are considered, with the goal of testing the robustness of implementation. Two meshes are tested: one containing 9390 elements and another with 14692 elements. The displacement at point (A) is shown in figure 5 for the two meshes. "Damping" is caused by the total stress law and electric field dispersion (boundaries allow normal electric flux). The contour plots of interested are shown in figure 6 for the finer mesh. The real deformed geometry is shown.

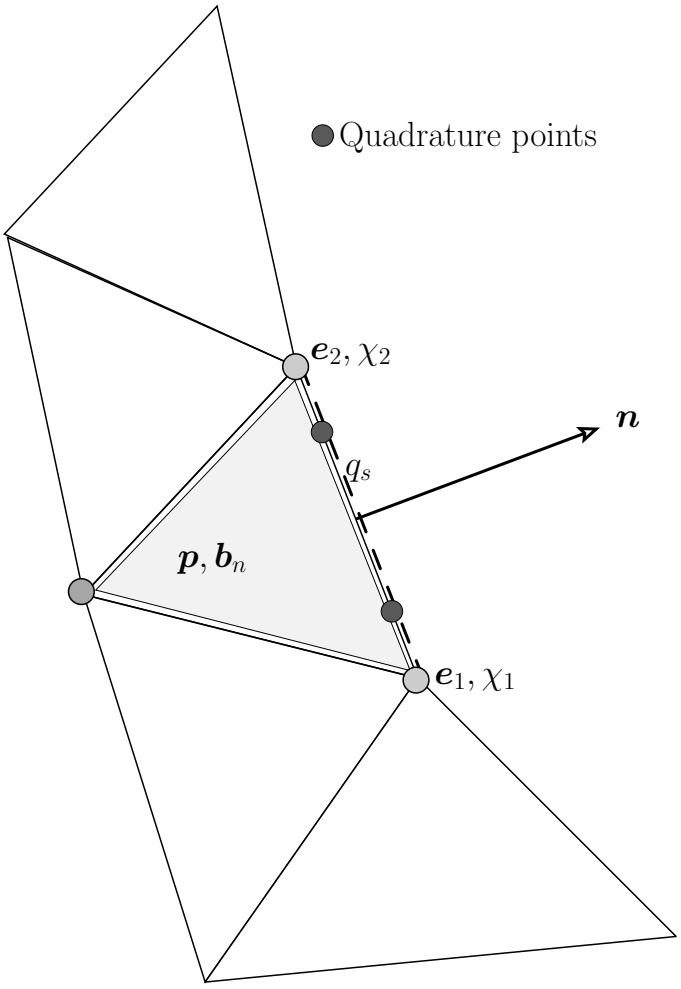


Figure 3: Boundary condition (31) for $\boldsymbol{e}$: use of a boundary element with Lagrange multipliers ($\chi_1$ and $\chi_2$).

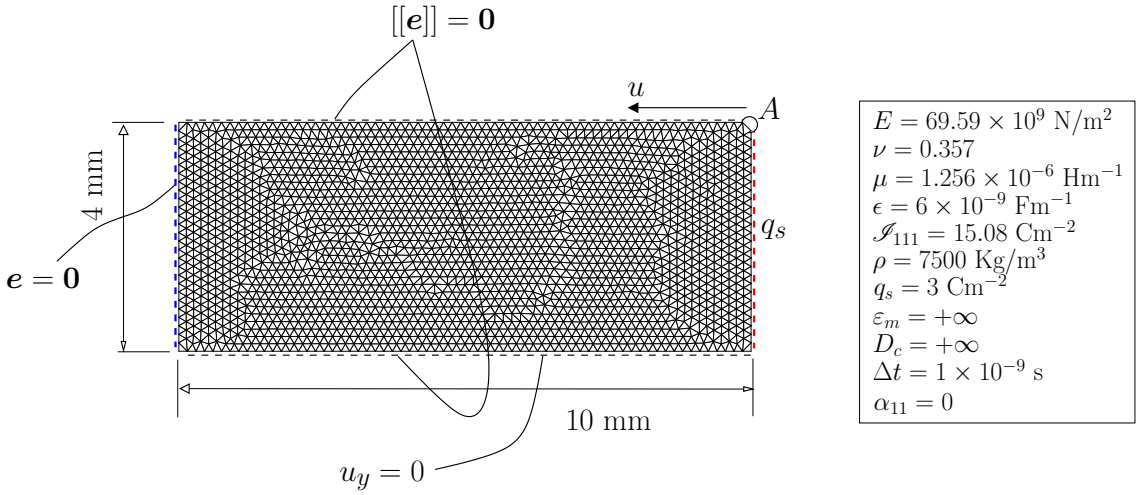


Figure 4: PZT specimen with relevant properties and dimensions. The (artificially coarse) mesh is shown for illustrative purposes only.

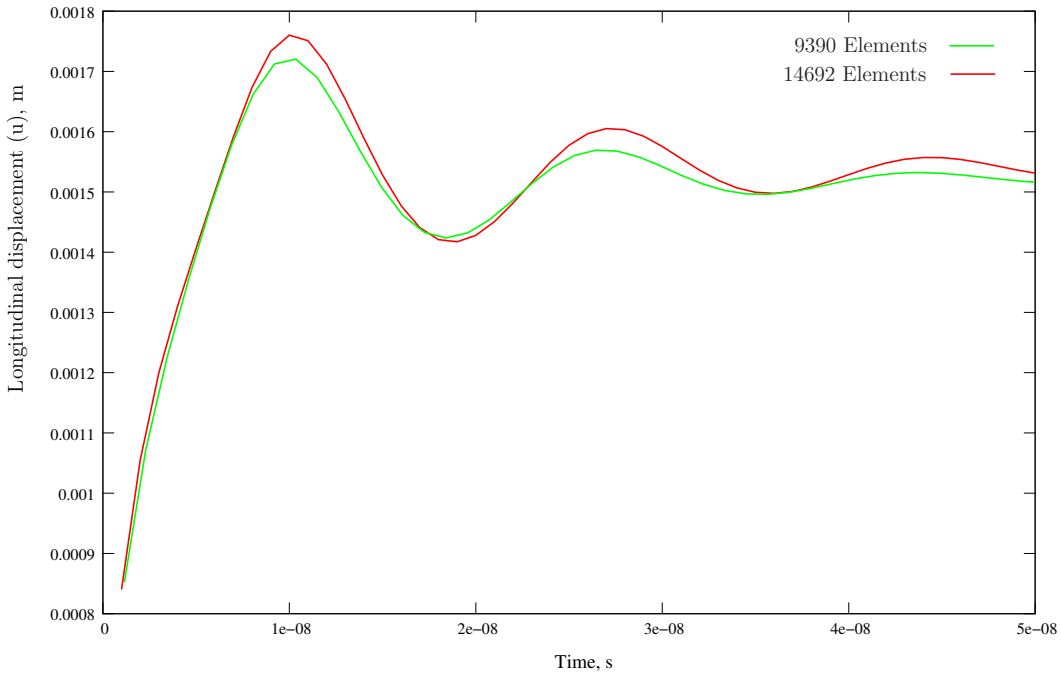


Figure 5: Displacement/time results for point $A$ for two mesh densities.

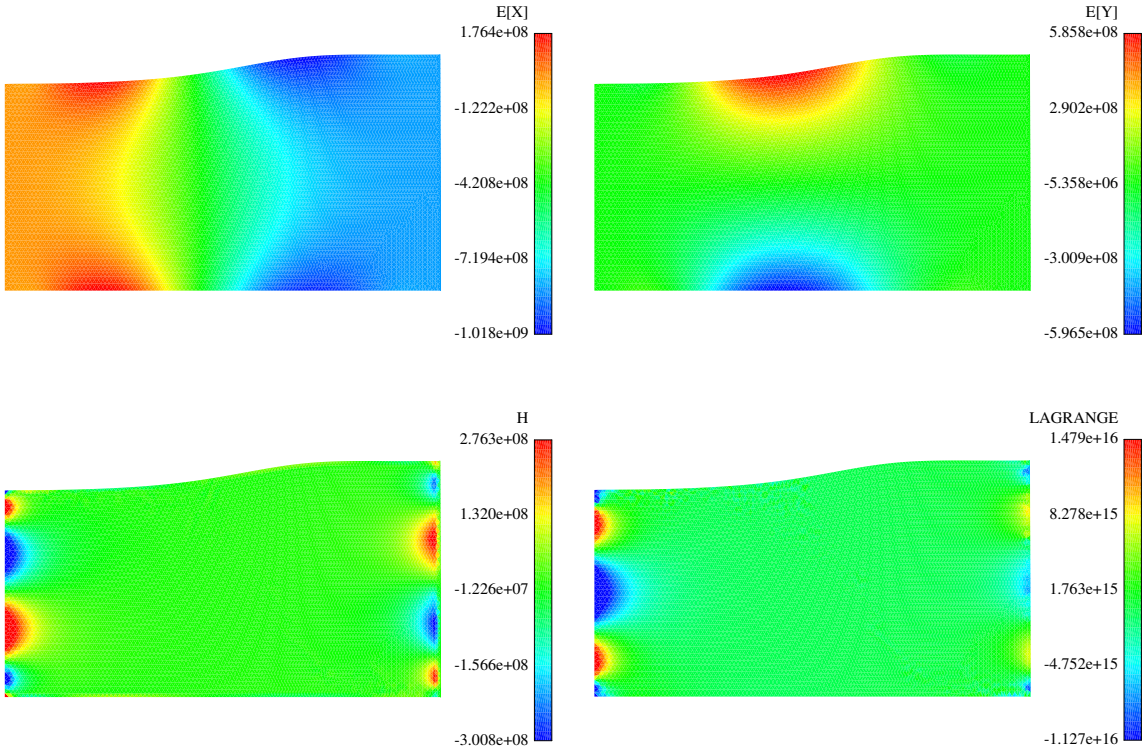


Figure 6: Electric ($\boldsymbol{e}$), magnetic ($\boldsymbol{h}$) and Lagrange multiplier ($\lambda$) fields for $t = 3.0 \times 10^{-8}$ s (not magnified).

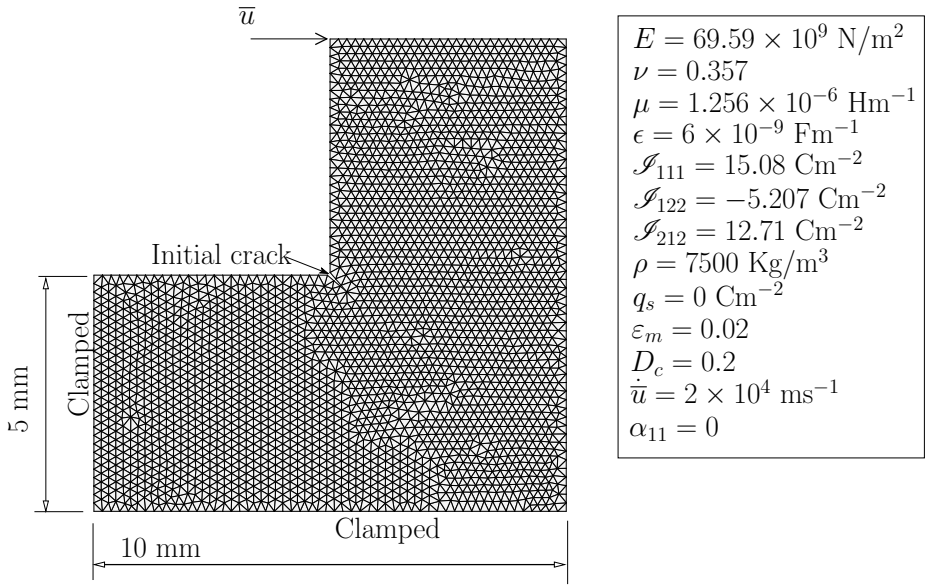


Figure 7: Corner crack: relevant data.

### 4.2 Corner crack evolution

The following problem is considered: a reentrant corner with a pre-existing 5 mm diagonal crack has two edges clamped and is subject to a constant velocity applied in a corner point. Figure 7 shows the relevant data of this problem. Again, a PZT material is considered with typical properties (except $\varepsilon_m$ and $D_c$ which are introduced here for verification purposes, a fact not affecting the conclusions). Three uniform-sized meshes are used to assert the sufficient independence of the results: 5268, 11824 and 26620 mixed triangular elements. The same time step of $\Delta t = 2 \times 10^{-10}$ s is used for all meshes. Besides the mechanical boundary conditions depicted in figure 7 the electric field is constrained with $q_s = 0$ Cm$^{-2}$. Now classical fracture algorithms (created by the first Author cf. [2, 4, 3]) are employed in this example with a *insulating* crack (see also [15]).

The reaction at the point of imposed displacement is monitored for the three meshes and the results are shown in figure 8. Close agreement occurs for the two finer meshes and very acceptable agreement is obtained in general. A comparison between the three crack paths is shown in figure 9 where excellent agreement can be observed. In addition, contour plots of relevant quantities for the finer mesh are shown in figure 10.

To inspect the effect of $\alpha_{11}$ in the crack path, we repeat the test for several values of $\alpha_{11}$ (0, $\pi/6$, $\pi/4$, $\pi/3$ and $\pi/2$) in figure 11. We can conclude, from the inspection of that figure, that, since the only source of anisotropy in our model is the piezoelectric law, it affects the crack path. There is a slightly crack path offset for $\alpha_{11} = \pi/3$.

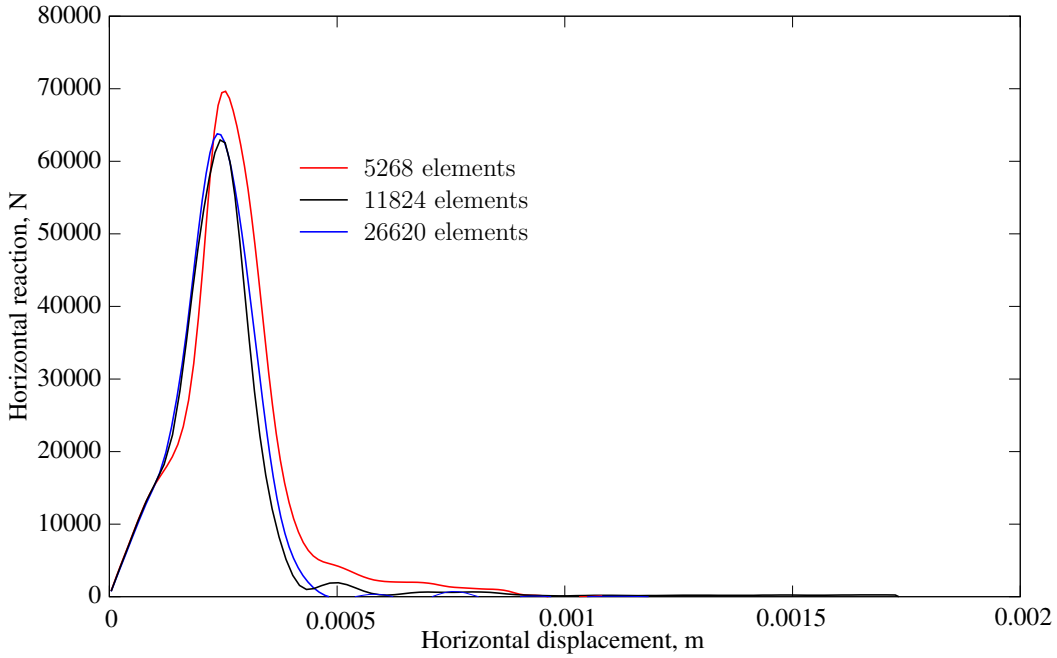


Figure 8: Load/displacement results for the corner crack problem, comparing the three meshes. 1 m depth is considered.

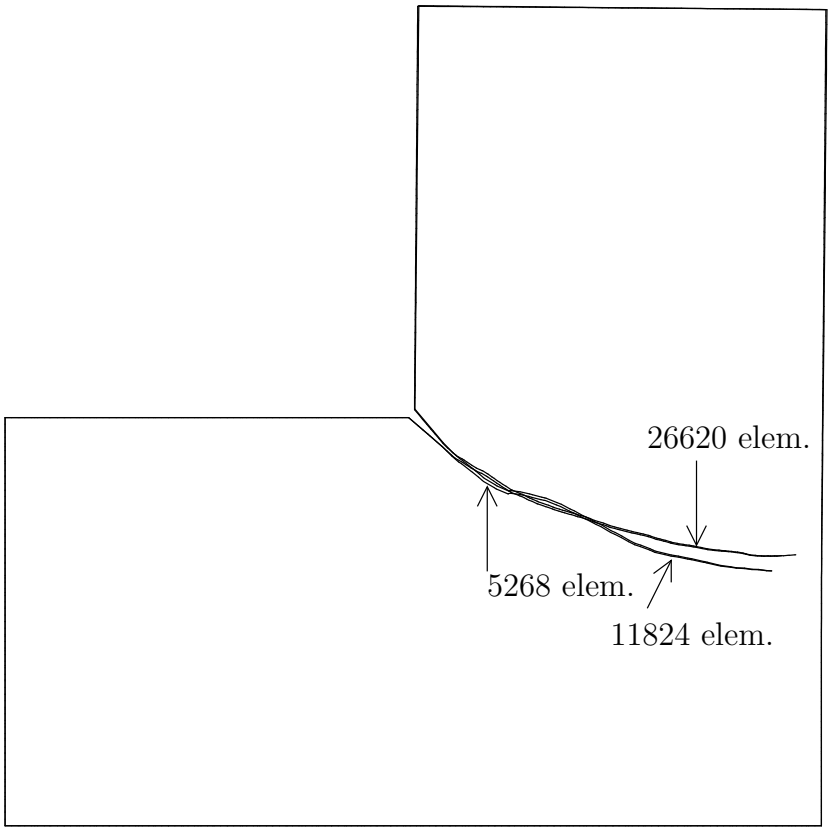


Figure 9: Crack path comparison between the three meshes

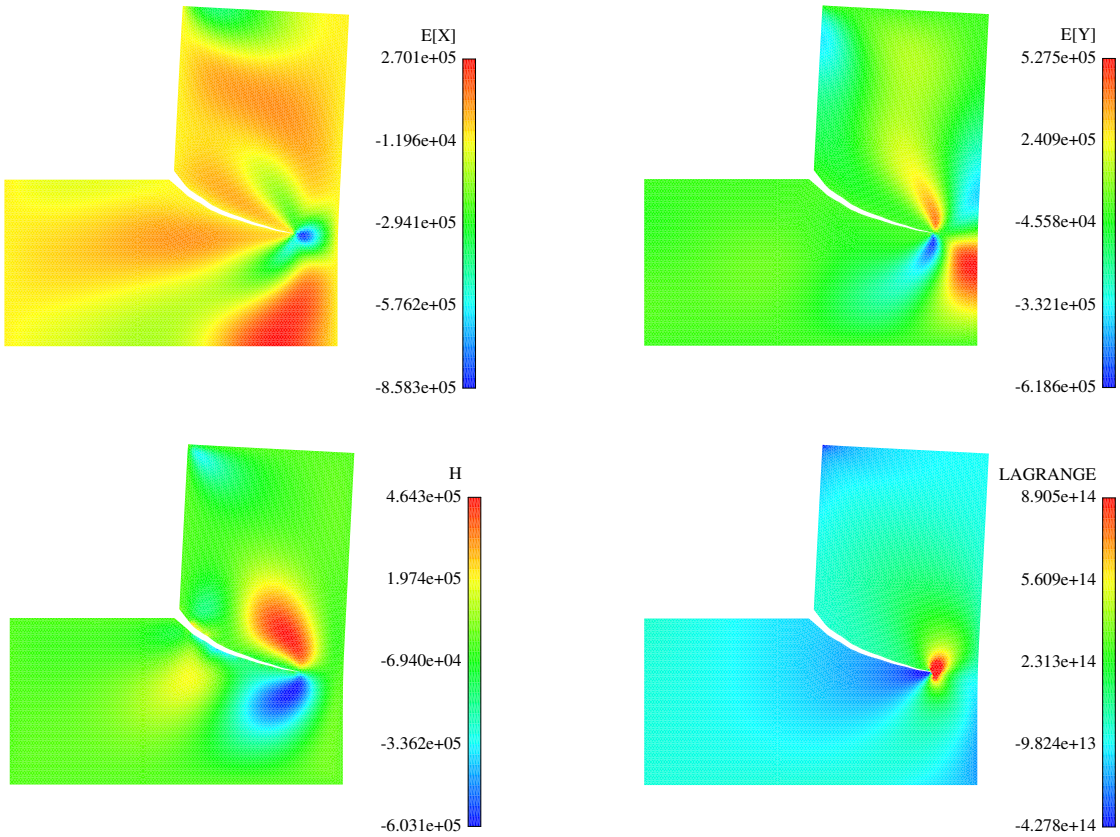


Figure 10: Electric ($\boldsymbol{e}$), magnetic ($\boldsymbol{h}$) and Lagrange multiplier ($\lambda$) fields for $t = 1.38 \times 10^{-8}$ s. For a clear representation of the crack path, the deformed geometry is $10\times$ magnified. The mesh containing initially 26620 elements is adopted.

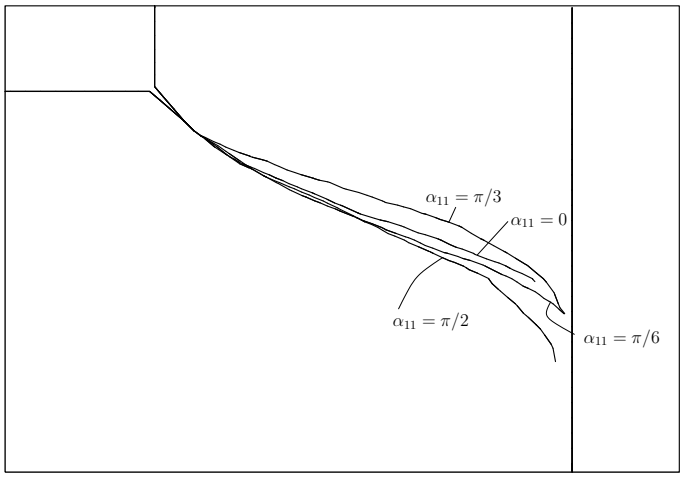


Figure 11: Effect of the piezoelectric angle $\alpha_{11}$ in the crack path.

# 5 Conclusions

Specialized derivations both in the strong and weak forms of electro-magnetic coupling of dielectrics including piezo-electricity were presented. New finite element formulations in both the continuum element (with a variant of the MINI element) and the boundary condition element were shown and two very successful numerical tests were presented. Compared with recent works on the same theme (e.g. [21]) the inclusion of the magnetic field, the derivation of novel electro-magnetic wave equations and the generalization of the boundary conditions were the major contributions. Further improvements in the number of ingredients and depth of numerical tests are being performed. The quality of implementation and corresponding results holds great promises for further generalization.

# Acknowledgments

The authors gratefully acknowledge financing from the "Fundação para a Ciência e a Tecnologia" under the Project PTDC/EME-PME/108751 and the Program COMPETE FCOMP-01-0124-FEDER-010267. The first author is grateful to Professor Philipe Geubelle and Dr. Scot Breitenfeld (University of Illinois) for several discussions and support of SIMPLAS ([1]).

## References


[1] P. Areias. Simplas. https://ssm7.ae.uiuc.edu:80/simplas.

[2] P. Areias, D. Dias-da-Costa, J. Alfaiate, and E. Júlio. Arbitrary bi-dimensional finite strain cohesive crack propagation. *Comput Mech*, 45(1):61–75, 2009.

[3] P. Areias, N. Van Goethem, and E.B. Pires. Constrained ale-based discrete fracture in shells with quasi-brittle and ductile materials. In *CFRAC 2011 International Conference*, Barcelona, Spain, June 2011. CIMNE.

[4] P. Areias, N. Van Goethem, and E.B. Pires. A damage model for ductile crack initiation and propagation. *Comput Mech*, 47(6):641–656, 2011.

[5] D.N. Arnold, F. Brezzi, and M. Fortin. A stable finite element for the Stokes equations. *Calcolo*, XXI(IV):337–344, 1984.

[6] A. Belahcen and K. and Fonteyn. On numerical modeling of coupled magnetoelastic problem. In T. Kvamsdal, K.M. Mathisen, and B. Pettersen, editors, *21 Nordic Seminar on Computational Mechanics*, NSCM, Barcelona, 2008. CIMNE, CIMNE.

[7] A. Dorfmann and R.W. Ogden. Nonlinear electroelastic deformations. *J Elasticity*, 82(2):99–127, 2006.

[8] J.L. Ericksen. On formulating and assessing continuum theories of electromagnetic fields in elastic materials. *J Elasticity*, 87:95–108, 2007.

[9] J.L. Ericksen. Theory of elastic dielectrics revisited. *Arch Ration Mech An*, 183:299–313, 2007.

[10] H.A. Haus and J.R. Melcher. *Electromagnetic Fields and Energy*. Prentice-Hall, 1989.

[11] T.J.R. Hughes. *The finite element method*. Dover Publications, 2000. Reprint of Prentice-Hall edition, 1987.

[12] J.D. Jackson. *Classical Electrodynamics*. John Wiley & Sons, Third edition, 1999.

[13] J. Korelc. Multi-language and multi-environment generation of nonlinear finite element codes. 18(4):312–327, 2002.

[14] M. Kuna. Finite element analyses of cracks in piezoelectric structures: a survey. *Arch Appl Mech*, 76:725–745, 2006.

[15] M. Kuna. Fracture mechanics of piezoelectric materials - Where are we right now? *Eng Fract Mech*, 77:309–326, 2010.

[16] M. Lax and D.F. Nelson. Maxwell equations in material form. *Physical Review B*, 13(4):1777–1784, 1976.

[17] J. Lemaitre. *A course on damage mechanics*. Springer, second edition, 1996.

[18] C. Linder, D. Rosato, and C. Miehe. New finite elements with embedded strong discontinuities for the modeling of failure in electromechanical coupled solids. *Comp Method Appl M*, 200:141–161, 2011.

[19] J.E. Marsden and T.J.R. Hughes. *Mathematical foundations of elasticity*. Dover Publications, 1994.

[20] G.A. Maugin. *Continuum mechanics of electromagnetic solids*, volume 33 of *Applied Mathematics and Mechanics*. North-Holland, 1988.

[21] A. Mota and J.A. Zimmerman. A variational, finite-deformation constitutive model for piezoelectric materials. *Int J Numer Meth Eng*, 85:752–767, 2011.

[22] R.W. Ogden. *Non-linear elastic deformations*. Dover Publications, Mineola, New York, 1997.

[23] P. Ponte Castañeda and M.H. Siboni. A finite-strain constitutive theory for electro-active polymer composites via homogenization. *International Journal of Non-Linear Mechanics*, 2011. In press.

[24] Wolfram Research Inc. Mathematica, 2007.

[25] D.K. Vu, P. Steinmann, and G. Possart. Numerical modelling of non-linear electroelasticity. *Int J Numer Meth Eng*, 70:685–704, 2007.